Matrix Metalloproteinases MMP2 and MMP9 Are Produced in Early Stages of Kidney Morphogenesis but Only MMP9 Is Required for Renal Organogenesis In Vitro

Brigitte Lelongt,* Germain Trugnan,‡ Gillian Murphy,§ and Pierre M. Ronco*

*Institut National de la Santé et de la Recherche Médicale, Unité 64, Hôpital Tenon, Paris, France; ‡Institut National de la Santé et de la Recherche Médicale, CJF 96-07, Faculté Saint-Antoine, Paris, France; and §Strangeways Research Laboratory, Cambridge, United Kingdom

Abstract. We analyzed matrix metalloproteinase (MMP) production by 11-d embryonic mouse kidneys and the effects of these enzymes on subsequent renal organogenesis. In vivo, immunolocalization of metalloproteinases by laser scanning confocal microscopy and zymograms of kidney lysates showed that the mesenchyme of embryonic kidneys synthesized both MMP9 and MMP2 enzymes. In vitro, embryonic kidneys also secreted both enzymes when cultured in a medium devoid of hormone, growth factor, and serum for 24 h during which T-shaped branching of the ureter bud appeared. We then evaluated the role of MMP2 and MMP9 in kidney morphogenesis by adding anti-MMP2 or anti-MMP9 IgGs to the culture medium of 11-d kidneys for 24 or 72 h. Although it inhibited activity of the mouse enzyme, anti-MMP2 IgGs had no effect on kidney morphogenesis. In contrast, anti-MMP9 IgGs with enzyme-blocking activity impaired renal morphogenesis, in a concentration-dependent manner, by inhibiting T-shaped branching and further divisions of the ureter bud. This effect was irreversible, still observed after inductive events and reproduced by exogenous tissue inhibitor of metalloproteinase 1 (TIMP1), the natural inhibitor of MMP9. These data provide the first demonstration of MMP9 and MMP2 production in vivo by 11-d embryonic kidneys and further show that MMP9 is required in vitro for branching morphogenesis of the ureter bud.

During mammalian embryonic development, interactions between epithelium and mesenchyme are required for the formation of differentiated epithelial sheets (Bard, 1990). The developing kidney is an excellent model to study these events, since renal organogenesis is characterized by reciprocal inductive interactions between an epithelial structure, the ureter bud, and a surrounding mesenchyme, the metanephric blastema. The interactions occur at the tips of the ureter bud, which undergoes branching morphogenesis during its penetration and growth in the metanephric blastema. They lead to the differentiation of a fraction of mesenchymal cells into epithelial cells. This phenotypic conversion is associated with the expression of extracellular matrix components that play a crucial role in the establishment of cell polarity and epithelial phenotype and in the branching morphogenesis of the ureter bud (Ekblom, 1993). In addition, a constant remodeling of the extracellular matrix is needed at the growing tips of the invading ureter bud to allow further branchings in the metanephric mesenchyme, which implies a role for matrix-degrading enzymes.

Matrix metalloproteinases are a large family of zinc requiring matrix-degrading enzymes, which include the interstitial collagenases, the stromelysins, and the type IV collagenases (Stetler-Stevenson et al., 1993). They have been implicated in invasive cell behavior and in embryonic development and morphogenesis. The genes encoding the stromelysins, the type IV collagenases, and the tissue inhibitors of metalloproteinases (TIMPs)[1] (Cawston et al., 1981; Goldberg et al., 1989; De Clerck et al., 1989; Apte et al., 1994) are activated from the early steps of mouse development throughout embryogenesis. An increase in the expression of metalloproteinases and TIMPs is observed at the blastocyst stage in invading trophoblastic cells during mouse embryo implantation (Brenner et al., 1989; Werb et al., 1992; Harvey et al., 1995; Reponen et al., 1995). Administration of metalloproteinase inhibitors retards decidual remodeling and growth (Alexander et al., 1996). Later on, these enzymes are still present in a variety of embryonic tissues (Nomura et al., 1989; Reponen et al., 1992, 1994; Apte et al., 1994; Lefebvre et al., 1995; Lim et al., 1995)

Address all correspondence to Brigitte Lelongt, Unité INSERM 64, Hôpital Tenon, 4 rue de la Chine, 75020 Paris, France. Tel.: (33) 1-40-30-65-14. Fax: (33) 1-40-30-62-17. e-mail: brigitte.lelongt@tnn.ap-hop-paris.fr

1. *Abbreviations used in this paper*: APMA, *p*-aminophenylmercuric acetate; DBA, dolichos biflorus agglutinin; HPA, helix pomatia agglutinin; MMP, matrix metalloproteinase; TIMP, tissue inhibitor of metalloproteinase; rhTIMP, recombinant human TIMP.

where their expression is correlated with a physiological role, especially in branching morphogenesis. An appropriate balance between metalloproteinases and their inhibitors is required in mammary gland development in virgin females and in its involution after lactation (Sympson et al., 1994; Talhouk et al., 1992). Matrix metalloproteinases (MMPs) also regulate branching of immature salivary glands, which was decreased by interstitial collagenases but increased by a collagenase inhibitor (Nakanishi et al., 1986), as well as lung branching, which was inhibited by enhanced MMP2 expression in response to exogenous TGFα and EGF (Ganser et al., 1991). No information, however, was available on the role of matrix metalloproteinases in ureter bud branching during renal organogenesis.

We speculated that these enzymes were produced in early stages of kidney morphogenesis and involved in the reciprocal inductive interactions that occur between epithelium and mesenchyme and lead to the branching of the ureter bud. To verify these hypotheses, we performed a two-step study that consisted of analyzing the production of metalloproteinases in 11-d mouse kidneys, and then of establishing the role of these enzymes by reducing their availability. The results show that MMP9 and MMP2 are produced in vivo at this stage of kidney development, and that MMP9 but not MMP2 is required in vitro for branching morphogenesis of the ureter bud.

Materials and Methods

Source and Characterization of Antibodies

We used previously described IgGs from anti–human MMP2 and anti–pig MMP9 sheep sera (Hipps et al., 1991; Murphy et al., 1989) and rabbit anti–human MMP9 antibody (Morel et al., 1993). Controls were IgGs from preimmune sheep serum and rabbit preimmune serum, respectively. Antibody solutions did not contain preservatives.

Immunoreactivity. To verify that the antibodies cross-reacted with mouse metalloproteinases, we performed Western blots with 24-h serum-free culture media from the mouse macrophage cell line RAW 264.7 and from the mouse fibroblast cell line NIH 3T3 (American Type Culture Tissue Collection, Rockville, MD), which secreted MMP9 and MMP2, respectively. Media were concentrated 10× with Microcon 30 concentrators (Amicon Inc., Beverly, MA), and Western blot (Fig. 1 *A*) was performed as described below. Rabbit anti–MMP9 antibody (Fig. 1, lanes *2* and *3*) and sheep anti–MMP9 IgGs (lanes *6* and *7*) reacted with mouse macrophage MMP9 (lanes *3* and *6*) but not with mouse fibroblast MMP2 (lanes *2* and *7*). Conversely, sheep anti–MMP2 IgGs (lanes *8* and *9*) recognized only mouse fibroblast MMP2 (lane *8*).

Inhibition of Enzymatic Activity. Mouse MMP2 purified from NIH 3T3 culture media by gelatin Sepharose chromatography and mouse recombinant MMP9 were preactivated with 2 mM *p*-aminophenylmercuric acetate (APMA; Sigma Chemical Co., St. Louis, MO) at 37°C for 1 h, and their activities were assayed using heat-denatured ^{14}C-type I collagen (Murphy et al., 1982). To test the inhibitory effect of antibodies on enzymatic activity, 0.6 U (1 U of enzyme degrades 1 mg of gelatin per min at 37°C) of mouse MMP2 or MMP9 was incubated with ^{14}C-type I collagen in the presence of increasing amounts of sheep anti–human MMP2 and anti–pig MMP9 IgGs, respectively, or of control sheep preimmune IgGs (Fig. 1 *B*). Results are expressed as the percentage of specific inhibition of the enzymatic activity. Specific inhibition was calculated by substracting values obtained with preimmune IgGs from those obtained with anti-MMP2 or anti-MMP9 IgGs. As shown in Fig. 1 *B*, the antibodies used in this study were able to specifically inhibit mouse MMP2 or MMP9 activities in a dose-dependent manner.

Organ Culture and Experimental Protocols

Kidneys were dissected from NMRI × C57/BL6 hybrid mice. The morning of the vaginal plug was defined as day 0 of gestation. To analyze the production of metalloproteinases in early kidney development, 11-d embryonic kidneys were grown in pairs for 24 h (37°C, 5% CO_2) on a 1-μm Nucleopore filter (Costar Corp., Cambridge, MA) floating on 50 μl of medium. This medium, changed daily, was composed of an equal volume of improved minimum essential medium (Richter et al., 1972) and Ham F12 (GIBCO BRL, Eragny, France) supplemented with 30 nM sodium selenate, 50 μg/ml transferrin, and 4 mM glutamine (Sigma Chemical Co.) (Ekblom et al., 1981), and was devoid of antibiotic, growth factor, hormone, and serum.

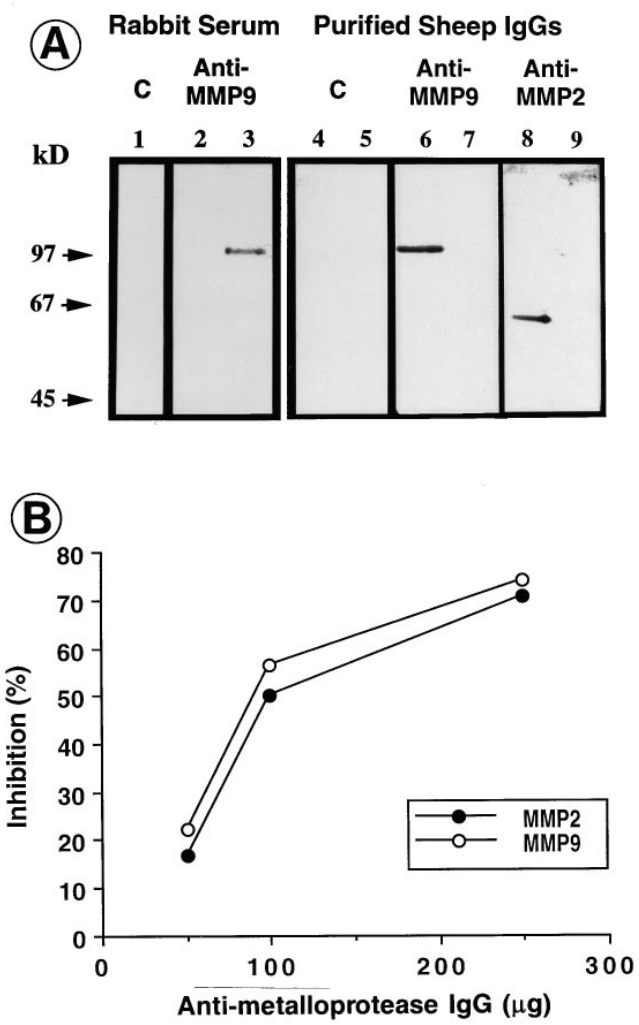

Figure 1. Antibody characterization. (*A*) Western blots performed with MMP9 (lanes *1*, *3*, *4*, *6*, and *9*) and MMP2 (lanes *2*, *5*, *7*, and *8*) isolated from mouse macrophage and NIH 3T3 cell lines, respectively. Rabbit anti–MMP9 antibody (lanes *2* and *3*) and sheep anti–MMP9 IgGs (lanes *6* and *7*) recognized mouse macrophage MMP9 (lanes *3* and *6*) but not mouse fibroblast MMP2 (lanes *2* and *7*). Conversely, sheep anti–MMP2 IgGs (lanes *8* and *9*) recognized mouse fibroblast MMP2 (lane *8*) but not mouse macrophage MMP9 (lane *9*). Neither rabbit preimmune serum (lane *1*) nor sheep preimmune IgGs (lanes *4* and *5*) reacted with mouse MMP9 (lanes *1* and *4*) or MMP2 (lane *5*). (*B*) The inhibitory effect of antibodies on enzymatic activity was estimated by incubating an aliquot (0.6 U) of MMP2 or MMP9 with heat-denaturated ^{14}C-type I collagen in the presence or absence of increasing amounts of sheep anti–MMP2 or anti–MMP9 IgGs or of sheep preimmune IgGs. Results are expressed as the percentage of specific inhibition of the enzymatic activity. The data points represent values obtained with anti–MMP2 or anti–MMP9 IgGs minus values obtained with preimmune IgGs.

In another set of experiments, we separately dissected by enzymatic treatment mesenchymes and ureter buds from 11-d kidneys. Kidneys were incubated first in 2.25% pancreatin, 0.75% trypsin in PBS, pH 7.4, for 80 s on ice, and then in culture medium containing 10% FCS for 1 h at room temperature. After five rinsings in culture medium devoid of serum, mesenchymes were separated from the ureter buds with disposable needles. The absence of metalloproteinase activity in the last wash was verified by zymography. Five ureter buds per filter and their corresponding mesenchymes were maintained separately for 24 h in the culture conditions described above.

To investigate the role of MMP2 and MMP9 in kidney morphogenesis, kidneys were cultured for 24 or 72 h in the culture medium described above supplemented with anti–MMP2 and anti–MMP9 antibodies or recombinant human TIMP1 (rhTIMP1) obtained from G. Abbott (Synergen, Boulder, CO). Isolated IgGs from anti–human MMP2 and anti–pig MMP9 sheep sera and rhTIMP1 were used at concentrations of 1–100 μg/ml. rhTIMP was first diluted in 2× HAM F12 since the volume of the solution was >5% of the culture medium. In control experiments, isolated sheep IgGs from preimmune serum served as a substitute for sheep anti–MMP2 and anti–MMP9 IgGs, and BSA for rhTIMP1.

Finally, we tested whether the effect of anti–MMP9 antibody could be reversed by growing 11-d kidneys for 24 h in the presence of sheep anti–MMP9 IgGs (1 μg/ml), and then by transferring them in medium supplemented with isolated sheep IgGs from preimmune serum (1 μg/ml) for 48 h, and whether it could still be observed after epithelial induction of the mesenchyme by culturing 11-d kidneys in the presence of preimmune sheep IgGs (1 μg/ml) for 24 h, and then in medium supplemented with sheep anti–MMP9 IgGs (1 μg/ml) for an additional 48 h.

All experiments were repeated at least 10 times.

Substrate Gel Electrophoresis (Zymography)

Tissue-associated and secreted metalloproteinases were detected and characterized by zymography (Heussen and Dowdle, 1980). This technique was applied to 20 solubilized 11-d kidneys, and to whole concentrated media pooled from two 11-d kidneys grown for 24 h in culture and from 30 11-d ureter buds or mesenchymes dissected separately and maintained in culture for 24 h. 11-d kidney explants were directly lysed in SDS-PAGE sample buffer (50 mM Tris, 1% SDS, 5% glycerol, 0.002% bromophenol blue). At this stage of development, embryonic kidneys are made of loose tissue that is totally solubilized under these conditions. Concentrated media were diluted in the same buffer to the above final concentrations. Solubilized kidneys and media were then loaded on 8% SDS polyacrylamide (Merck, Darmstadt, Germany) gels copolymerized with 1 mg/ml of gelatin or type IV collagen (Sigma Chemical Co.). Electrophoresis was performed under nonreducing conditions at 20 mA for 2 h at 4°C. Gels were washed twice for 30 min in 2.5% Triton X-100 to remove SDS, incubated in substrate buffer (50 mM Tris-HCl, 5 mM $CaCl_2$, 1 μM $ZnCl_2$, 0.01% NaN_3, pH 7.5) for 24 h at 37°C, stained in 0.5% Coomassie blue (prepared in 30% ethanol, 10% acid acetic, 1% formaldehyde) for 30 min at room temperature, and destained three times for 15 min in the same buffer devoid of Coomassie blue and enriched in formaldehyde to 5%. The presence of metalloproteinases was indicated by an unstained proteolytic zone of the substrate. Both active and inactive proenzymatic forms are revealed by this technique because exposure of proenzyme to SDS during gel separation procedures leads to activation without proteolytic cleavage (Hipps et al., 1991). In some experiments, the active forms of metalloproteinases were induced by incubating the samples with APMA (1 mM) for 3 h at 37°C.

To characterize the metalloproteinases produced by embryonic kidneys according to their sensitivity to specific inhibitors, we performed SDS substrate gel electrophoresis with concentrated media from two 11-d kidneys grown for 24 h as described above, except that metalloproteinase inhibitors (10 mM EDTA, 1 mM 1,10 phenanthroline) were added to the samples before electrophoresis and supplied again in the substrate buffer. In addition, because metalloproteinases require calcium ions to be active, the ability of these enzymes to create zones of lysis was tested when calcium ion was replaced by another divalent cation as Mg^{2+} (5 mM) or Mn^{2+} (5 mM) in the substrate buffer.

Immunoblotting

MMP2 and MMP9 were identified in 24-h concentrated media from 16 and 50 11-d kidneys, respectively, submitted to SDS-PAGE under nonreducing conditions in an 8% polyacrylamide gel, and electrotransferred to nitrocellulose (Schleicher and Schuell, Darmstadt, Germany) for 2 h at a constant current of 190 mA. Afterwards, nitrocellulose sheet was saturated with 5% dry milk in 0.1% PBS-Tween for 1 h at 37°C, extensively washed in 0.1% PBS-Tween, and incubated overnight at 4°C with one of the following antibodies: sheep anti–MMP2 IgGs or preimmune IgGs as control (4 μg/ml), rabbit anti–MMP9 antibody or preimmune serum as control (dilution 1:250). Nitrocellulose was then incubated for 2 h at room temperature with anti–sheep or anti–rabbit IgGs, respectively, conjugated to alkaline phosphatase (0.02 μg/ml; Amersham, Les Ullis, France). Alkaline phosphatase activity was revealed by adding the NBT/BCI substrate (nitro blue tetrazolium/5-bromo-4-chloro-3-indolyl phosphate complex in 100 mM Tris-HCl, 100 mM NaCl, and 5 mM $MgCl_2$, pH 9.5). The reaction was stopped in 20 mM Tris-HCl and 5 mM EDTA, pH 8.0.

Immunomorphological Studies

Whole Mount Laser Scanning Confocal Microscopy. It was performed on 11-d kidneys to establish the in vivo localization of MMP2 and MMP9. Kidneys were sampled from embryos of pregnant mice at 11 d of gestation, immediately fixed with 4% paraformaldehyde in PBS, pH 7.4, for 30 min at room temperature, and further incubated for 10 min in NH_4Cl. They were then saturated with 10% FCS diluted in PBS supplemented with 0.075% saponin detergent that was added throughout the labeling procedure. Afterwards, they were incubated overnight at 4°C in primary antibody diluted in saponin-PBS supplemented with 5% FCS. Sheep anti–MMP2 and control sheep preimmune IgGs were used at 100 μg/ml; rabbit anti–MMP9 antibody and control preimmune serum were used at 1:300 dilution. After several washes in saponin-PBS, kidneys were then incubated for 2 h at room temperature in saponin-PBS containing FITC-conjugated anti–rabbit IgG antibody (dilution 1:300) (Biosys, Compiègne, France) or anti–sheep IgG antibody (dilution 1:75) (Southern Biotechnology Associates Inc., Birmingham, AL) and rhodamine TRITC-conjugated helix pomatia agglutinin (HPA) and dolichos biflorus agglutinin (DBA) lectins (6 μg/ml; Sigma Chemical Co.) to localize the ureter bud. In some experiments, lectin staining was omitted and nuclei were stained with propidium iodide after incubation with the antibodies. For this purpose, kidneys were treated with RNAse A (1 mg/ml) for 10 min, and then incubated in propidium iodide (0.05 μg/ml) diluted in saponin-PBS for another 10 min. After a series of additional washes, kidneys were then mounted in glycerol and viewed under a Leica TCS laser scanning confocal microscope equipped with DMR inverted microscope (Heerbrugg, Switzerland). Excitation bands for FITC (488 nm) and rhodamine (568 nm) were generated by an argon-krypton laser. FITC staining was recovered through a band-pass filter that cut light over 590 nm, whereas TRITC staining was recovered through a long-pass filter adjusted to recover 90% of the red signal. FITC and rhodamine double-labeled specimens were analyzed either sequentially or in one pass with cross correction to suppress injection from one channel to another. Pinhole size was adjusted at 30% of the maximal aperture and was not modified thoughout analysis. Optical sections through embryonic kidneys were performed either in planes parallel (x-y plane) or perpendicular (x-z plane) to the plane of the ureter bud. Scanware® software was used to store, calculate, and combine images that were directly shot from the screen through a Focus Plus® camera on Kodak Elite 100 films (Eastman Kodak Co.). Alternatively, confocal images were transferred to Power Macintosh (Apple Computer Co., Cupertino, CA), prepared for printing through Photoshop® (Adobe Systems, Inc., Mountain View, CA), and finally printed on an XLS 8600 PS printer (Eastman Kodak Co.).

Whole Mount Direct Immunofluorescence. In experiments testing the effects of anti–MMP2 and anti–MMP9 IgGs on kidney morphogenesis, antibody penetration into renal tissue was also assessed by direct whole mount immunofluorescence. 11-d kidneys grown for 72 h in medium supplemented with anti–MMP2 or anti–MMP9 IgGs were fixed with 4% paraformaldehyde and processed as described above except that the first incubation step with primary antibodies was omitted. They were then mounted in glycerol and viewed under a microscope (E. Leitz, Inc., Rockleigh, NJ).

Results

Production of Metalloproteinases by 11-d Kidneys in Organotypic Culture

We first verified that 11-d kidneys grown for 24 h in medium devoid of hormone, growth factors, and FCS differentiated properly. They indeed did so since we observed

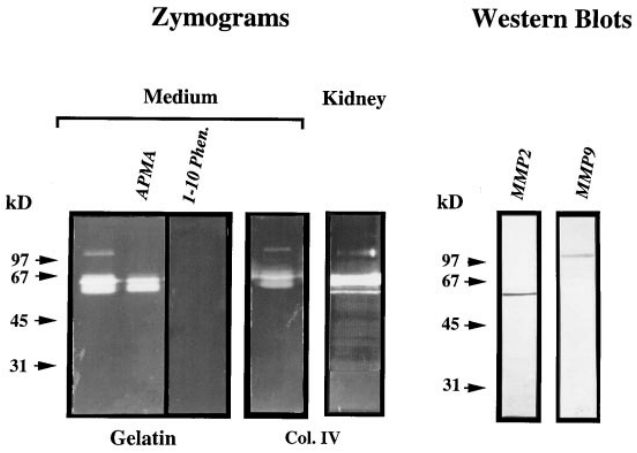

Figure 2. Identification of matrix metalloproteinases produced by 11-d kidneys by gelatin and type IV collagen gel electrophoresis (zymograms) and by Western blotting. Zymograms were performed in 8% polyacrylamide gels containing 1 mg/ml of gelatin or type IV collagen (*Col. IV*), with whole concentrated media from two kidneys grown for 24 h in culture (*Medium*) or with 20 kidney explants directly solubilized in SDS-PAGE sample buffer (*Kidney*). Note the presence, in whole concentrated media, of a lytic band at 102 kD and of a doublet at 64 and 60 kD in gelatin and in collagen gels. The same bands were observed in the lysate of 20 kidney explants (*Kidney*). The lytic profile was substantially modified by APMA and disappeared in the presence of 1,10 phenanthroline (*1-10 Phen.*). Western blots, performed with specific rabbit anti–MMP9 antibody (dilution 1:250) and sheep anti–MMP2 IgGs (4 μg/ml) on 24-h whole concentrated media from 16 kidneys for MMP2 and from 50 kidneys for MMP9, identified the 102- and 60-kD bands as MMP9 and MMP2, respectively. Controls with rabbit preimmune serum and sheep preimmune IgGs at the same concentrations were negative (not shown).

appropriate T-shaped branching of the ureter bud with condensed mesenchymal cells around the tips (data not shown).

Gelatin and type IV collagen gel electrophoresis of whole concentrated media from two kidneys showed one lysis band at 102 kD and a doublet at 60 and 64 kD (Fig. 2). When lower amounts of concentrated media were applied, the 60-kD band then resolved into a doublet (not shown). In all cases, the 64-kD band was predominant. After incubation with APMA, an organomercurial compound that specifically cleaves inactive forms of metalloproteinases, the 102-kD band disappeared and two major bands were observed at 64 and 60 kD, the 60-kD band being then more intense than that of 64 kD (Fig. 2). No lytic band appeared in the presence of 1,10 phenanthroline (Fig. 2), EDTA (data not shown), or when calcium ion was replaced by another divalent cation as Mg^{2+} (5 mM) or

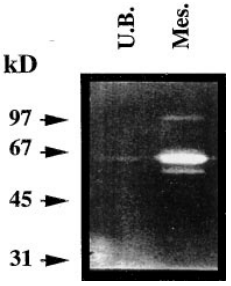

Figure 3. Zymography of ureter bud and mesenchyme concentrated media. 11-d ureter buds and mesenchymes were dissected apart and maintained separately for 24 h in culture. Gelatin-gel zymograms were performed with whole concentrated media from 30 ureter buds and their corresponding mesenchymes. Note that both MMP9 (102 kD) and the inactive (64 kD) and active (60 kD) forms of MMP2 were observed in mesenchyme concentrated medium (*Mes.*), while only a faint 60-kD band was detected in ureter bud concentrated medium (*U.B.*).

Mn^{2+} (5 mM) in the substrate buffer (data not shown). Moreover, the lytic pattern was identical in gelatin and type IV collagen gels, which suggested that the gelatinolytic activity was due to type IV collagenases.

Identification of the type IV collagenases was achieved by Western blotting performed on 24-h whole concentrated media from 16 kidneys for MMP2 and from 50 kidneys for MMP9. The rabbit anti–MMP9 antibody recognized only one 102-kD antigen corresponding to the proenzymatic form of MMP9 (Reponen et al., 1994). The same reactivity was observed with the sheep anti–MMP9 IgGs (not shown). We could not detect bands with lower molecular masses corresponding to active forms of MMP9 with any of the two antibodies, probably because of the low amount of MMP9 antigen and of the rapid degradation of the enzyme during activation (Okada et al., 1992). The sheep anti–MMP2 IgGs reacted with a single band at 60 kD corresponding to the active form of MMP2, i.e., the major lytic form observed by zymography after APMA cleavage of the 64-kD proenzyme (Fig. 2). Taken as a whole, these results show that cultured 11-d kidneys produce proenzymatic forms of MMP2 and MMP9 and active MMP2 enzyme. It was not possible to directly demonstrate active forms of MMP9.

To investigate the respective contribution of ureter bud and mesenchyme to MMP9 and MMP2 production, 11-d ureter buds and mesenchymes were dissected apart and maintained separately in culture for 24 h. Zymograms performed on 24-h whole concentrated media from 30 ureter buds and mesenchymes showed that, in 11-d kidneys, the mesenchyme was responsible for the production of both enzymes (Fig. 3).

In Vivo Expression of MMP9 and MMP2 in 11-d Kidneys

MMP9 and MMP2 expression was confirmed in vivo, in

Figure 4. Immunolocalization of MMP2 in whole mount 11-d kidneys by laser scanning confocal microscopy. Kidneys from 11-d embryos were incubated with sheep anti–MMP2 IgGs (100 μg/ml) (*G–O*) or control sheep preimmune IgGs (*A–F*) that were revealed by a second antibody conjugated to FITC. HPA and DBA lectins linked to rhodamine (6 μg/ml) were used to localize the ureter bud (*white arrows* in *E*, *H*, and *K*), although they also give a background staining of the mesenchyme. (*A–L*) Representative sections (2-μm-depth each) corresponding to top, middle, and bottom sections of 11-d kidneys were optically generated in planes parallel to that of the ureter bud (x-y plane). (*A–C* and *G–I*) FITC staining by antibodies; (*D–F* and *J–L*) merge pictures resulting from double staining by antibodies and lectins. Specific MMP2 staining (*G–L*) is observed in the mesenchyme throughout the kidney from the superficial (*Top*) to the inner (*Bottom*) areas, as shown by FITC staining (*G–I*) or double immunofluorescent stainings (*J–L*), compared with the negative control sheep IgG staining (*A–F*). (*M*) Higher magnification of a section shown in *K* labeled with anti–MMP2 IgGs and lectins exhibited a predomi-

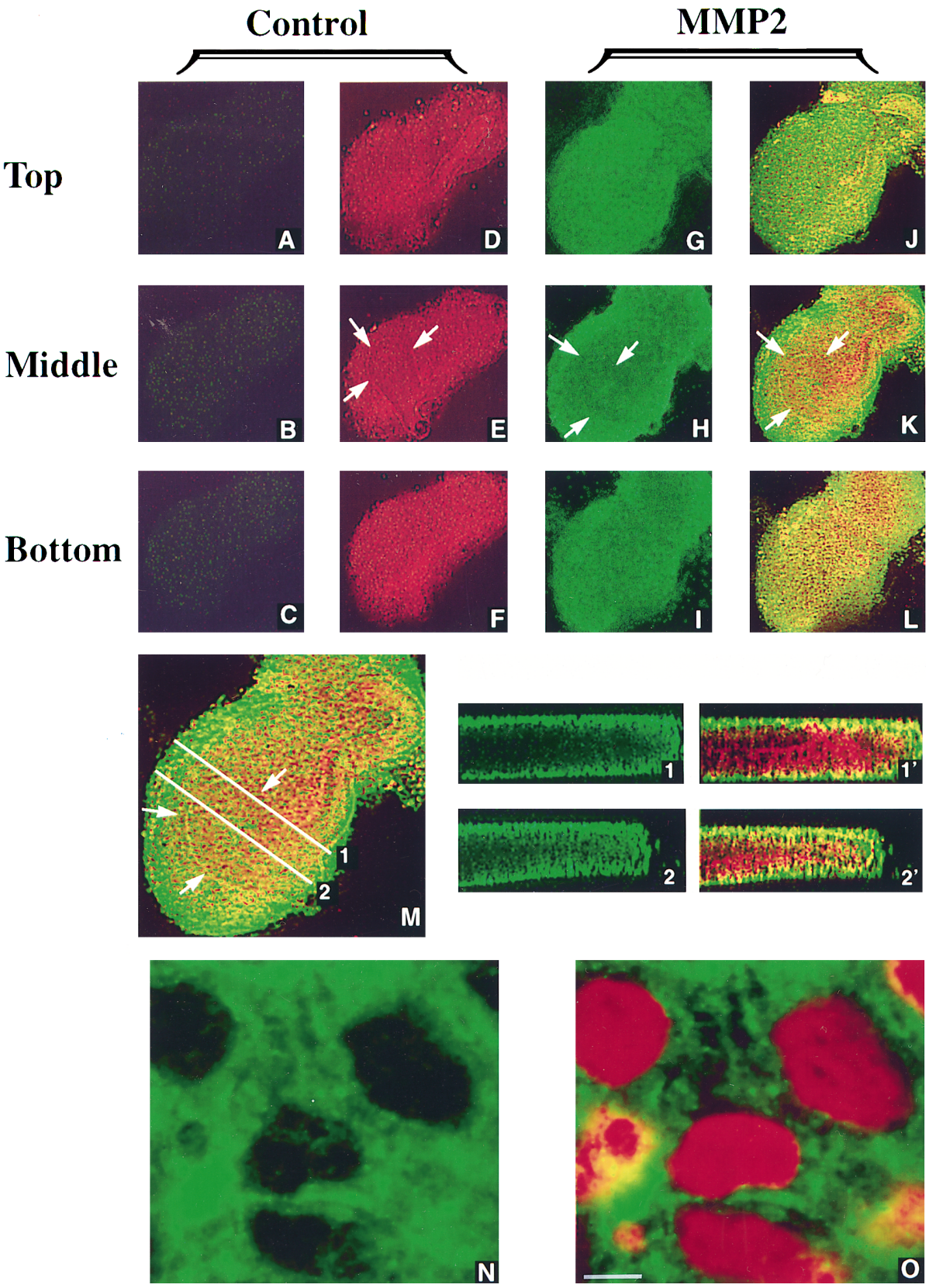

nant staining in the mesenchymal cells compared with the ureter bud. This is further illustrated by sections *1* and *2* optically generated in a plane perpendicular to that of the ureter bud (x-z plane). *1* and *2* represent MMP2 labeling; *1′* and *2′* represent the merge picture resulting from double staining with lectins to localize the ureter bud in red. (*N–O*) Cells labeled with sheep anti–MMP2 IgGs (*N*) and counterstained with propidium iodide to localize the nuclei in red (*O*) exhibited a cytoplasmic, vesicular and perinuclear staining. Bar: (*A–L*) 220 μm; (*M*) 130 μm; (*1*, *1′*, *2* , *2′*) 67 μm; (*N* and *O*) 8 μm.

11-d kidneys, by zymography and laser confocal microscopy. First, lysates from 20 kidneys analyzed by type IV collagen zymography (Fig. 2, *Kidney*) produced lysis bands corresponding to MMP9 (102 kD) and to MMP2 (64 and 60 kD). Second, laser confocal microscopy demonstrated the expression of MMP2 (Fig. 4) and MMP9 (Fig. 5) antigens in whole mount 11-d kidneys. Sections (2-μm-depth each) were optically generated in successive planes parallel to that of the ureter bud (x-y plane) from the superficial (*top*) to the inner (*bottom*) areas of the kidney and through the ureter bud (*middle*). MMPs were detected using FITC-conjugated second antibody, and HPA and DBA lectins

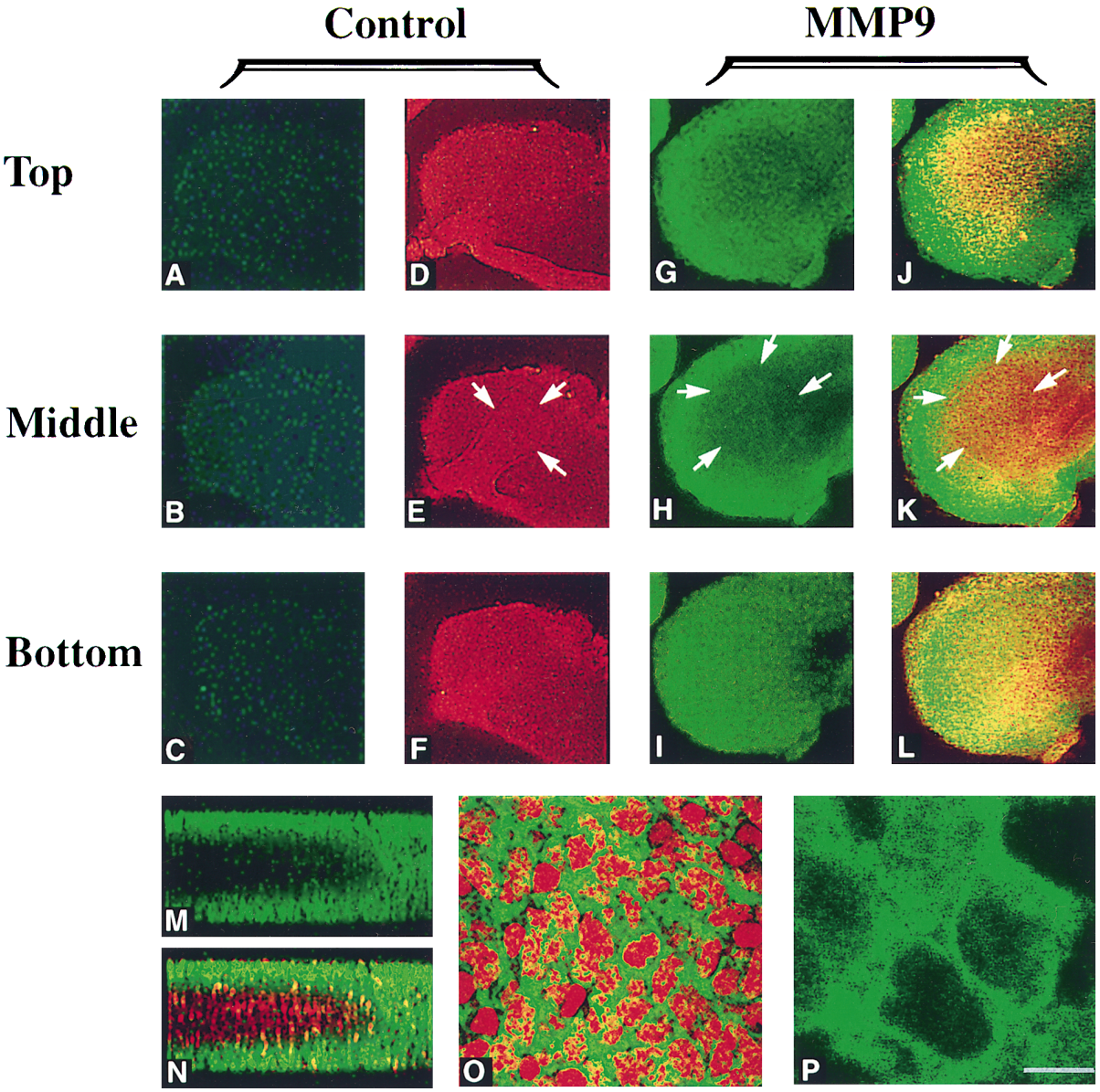

Figure 5. Immunolocalization of MMP9 in whole mount 11-d kidneys by laser scanning confocal microscopy. MMP9 was detected using anti–MMP9 rabbit antibody and FITC-conjugated anti–rabbit IgGs. HPA and DBA lectins linked to rhodamine (6 μg/ml) were used to localize the ureter bud (*white arrows* in *E*, *H*, and *K*). Rabbit preimmune serum (*A–F*) served as control for rabbit anti–MMP9 antibody (dilution 1:300) (*G–P*). (*A–L*) Representative sections (2-μm-depth each) corresponding to top, middle, and bottom sections of 11-d kidneys were optically generated in planes parallel to that of the ureter bud (x-y plane). (*A–C* and *G–I*) FITC staining by antibodies; (*D–F* and *J–L*) merge pictures resulting from double staining by antibodies and lectins. Staining in control kidneys incubated with rabbit preimmune serum (*A–F*) was negative. In contrast, specific MMP9 labeling (*G–L*) was observed in the mesenchyme from the superficial (*Top*) to the inner (*Bottom*) areas of the kidney, as illustrated by FITC (*G–I*) or double immunofluorescent (*J–L*) stainings. The middle section through the plane of the ureter bud (*H* and *K*) showed that MMP9 is expressed in the mesenchyme only. (*M* and *N*) Sections generated in a plane perpendicular to that of the ureter bud (x-z plane) stained with FITC (*M*) or double stained (*N*) further illustrated that MMP9 is expressed by mesenchymal cells in close contact with the ureter bud labeled with lectins linked to rhodamine, but not in this structure. (*O* and *P*) Cells were labeled with anti–MMP9 antibody (*P*) and counterstained with propidium iodide (*O*). (*P*) Section generated with an electronic fourfold zoom. Note that MMP9 staining is cytoplasmic and perinuclear. Bar: (*A–L*) 220 μm; (*M* and *N*) 130 μm; (*O*) 46 μm; (*P*) 10 μm.

linked to rhodamine were used to localize the ureter bud. 11-d kidneys incubated with sheep anti–MMP2 IgGs (Fig. 4, *G–L*) or with rabbit anti–MMP9 antibody (Fig. 5, *G–L*) exhibited a specific mesenchymal staining compared with control kidneys treated with preimmune sheep IgGs (Fig. 4, *A–F*) or with preimmune rabbit serum (Fig. 5, *A–F*), respectively. Merge picture resulting from double staining with antibodies and lectins suggested that MMP2 (Fig. 4, *J–L*) and MMP9 (Fig. 5, *J–L*) expression was intense in mesenchymal cells and negative or very faint in the ureter bud (Figs. 4 *K* and 5 *K*, respectively). This was further illustrated by sections generated in a plane perpendicular through the ureter bud (x-z plane). Representative sections through the ureter bud showed that MMP9 staining, identified by the green FITC labeling (Fig. 5 *M*), was not localized in the ureter bud labeled with rhodamine-conjugated lectins but was restricted to the surrounding mesenchyme on each side (Fig. 5 *N*). MMP2 localization was similar, although a faint ureter bud staining cannot be excluded (Fig. 4 *M*, *1* and *1′*, *2* and *2′*). Mesenchymal cells stained with anti–MMP2 IgGs (Fig. 4 *N*) or anti–MMP9 antibody (Fig. 5 *P*) and counterstained with propidium iodide to localize the nuclei in red (Figs. *4 O* and *5 O*, respectively) exhibited an intracytoplasmic, vesicular and perinuclear immunofluorescence excluding cell membranes and nuclei, irrespective of their localization in the superficial or inner areas of the kidney.

Since in vivo and in vitro studies on MMP2 and MMP9 production by 11-d kidneys provided similar results, we considered that the organotypic culture model was appropriate to investigate the role of these enzymes in kidney morphogenesis.

Role of MMP2 and MMP9 in Kidney Morphogenesis

To address this question, 11-d kidneys were cultured for 24 or 72 h in the presence of either sheep anti–MMP2 IgGs or sheep anti–MMP9 IgGs added to culture medium. Antibody penetration in tissue was demonstrated by direct immunofluorescence of kidneys with FITC-linked anti–sheep IgGs to localize anti–MMP2 and anti–MMP9 antibody, respectively (data not shown).

Anti–MMP2 IgGs, which specifically inhibit the enzymatic activity (Fig 1 *B*), had no effect on kidney morphogenesis (Fig. 6) even at 100 μg/ml. Indeed, similar ureter bud branching was observed in antibody-treated kidneys (Fig. 6, *B* and *D*) and in control kidneys incubated with sheep preimmune IgGs at the same concentration (Fig. 6, *A* and *C*) after 24 h (Fig. 6, *B* vs *A*) and 72 h in culture (Fig. 6, *D* vs *C*).

In contrast, anti–MMP9 antibody markedly impaired renal morphogenesis. Fig. 7 shows the effects of 1 μg/ml sheep anti–MMP9 IgGs on 11-d kidneys. No T-shaped branching of the ureter bud was visible after 24 h (Fig. 7 *B*), and further branching was markedly reduced after 72 h (Fig. 7 *D*) compared with control kidneys incubated with sheep preimmune IgGs (Fig. 7, *A* and *C*). The impairment of ureter bud branching after 72 h in culture was concentration dependent (Fig. 8 and Table I). Total inhibition was observed at 10 μg/ml of sheep anti–MMP9 IgGs, whereas control sheep IgGs had still no effect at this concentration.

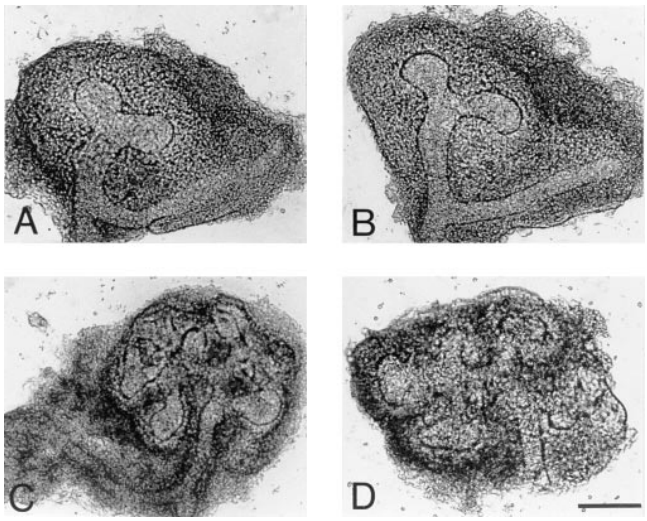

Figure 6. Morphology of sheep control (*A* and *C*) and anti–MMP2 IgG-treated (*B* and *D*) 11-d kidneys grown for 24 (*A* and *B*) or 72 h (*C* and *D*) in culture. Sheep preimmune and anti–MMP2 IgGs were added to culture media of 11-d kidneys at a concentration of 100 μg/ml. Note that anti–MMP2 IgGs had no effect on kidney morphogenesis since ureter bud branching was similar in control (*A* and *C*) and antibody-treated kidneys (*B* and *D*) after 24 (*A* vs *B*) and 72 h (*C* vs *D*) in culture. Pictures of whole mount kidneys are representative of 10 experiments. Bar: (*A* and *B*) 125 μm; (*C* and *D*) 200 μm.

These alterations were not reversible since ureter bud branching was similar in 11-d kidneys grown in medium supplemented with sheep anti–MMP9 IgGs (1 μg/ml) for 24 h only (Fig. 9 *A*), and in the same antibody-treated kidneys that were allowed to differentiate further by transfer for an additional 48 h in control medium supplemented with sheep preimmune IgGs (Fig. 9 *B*). Ureter bud branching was also impaired when 11-d kidneys were first allowed to differentiate for 24 h in control medium before being incubated with the antibody (1 μg/ml) for the next 48 h (Fig. 9, *D* vs control conditions shown in *C*). Finally, inhibition of ureter bud branching was observed in kidneys sampled at day 12 and treated with the anti–MMP9 IgGs (1 μg/ml) for 24 and 72 h (data not shown).

To confirm the involvement of MMP9 in ureter bud morphogenesis, we asked whether TIMP1, the natural inhibitor of MMP9, could reproduce the alterations observed with anti–MMP9 antibody. When 11-d kidneys were grown for 72 h in the presence of rhTIMP1, ureter bud branching was impaired in a concentration-dependent manner compared with control kidneys incubated with the same concentration of BSA (Fig. 10 and Table I). Total inhibition occurred at 10 μg/ml.

Discussion

In this work, we first show that the two type IV collagenases, MMP2 and MMP9, are produced by the mesenchyme of 11-d kidneys at the time of reciprocal inductive interactions between the ureter bud and the metanephric mesenchyme. In addition, we provide the first evidence that MMP9 is required in vitro for the first T-shaped divi-

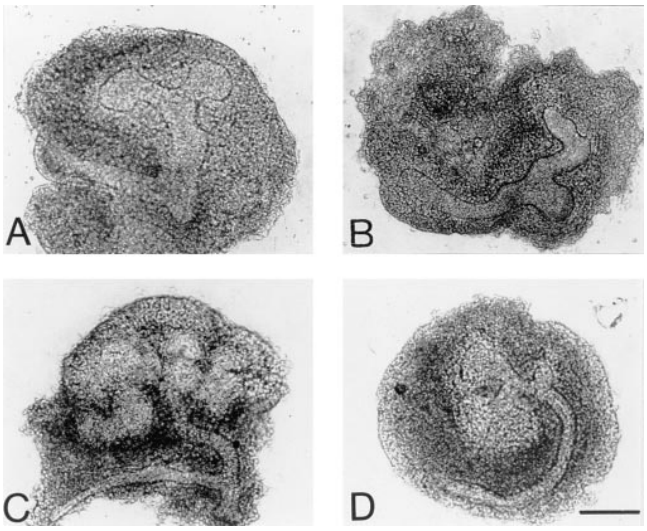

Figure 7. Morphology of sheep control (*A* and *C*) and anti–MMP9 IgG-treated (*B* and *D*) 11-d kidneys grown for 24 (*A* and *B*) or 72 h (*C* and *D*) in culture. Sheep preimmune and anti–MMP9 IgGs were added to culture media of 11-d kidneys at a concentration of 1 μg/ml. In anti–MMP9 IgG-treated kidneys, T-shaped branching of the ureter bud was totally inhibited after 24 h in culture (*B*), and branching morphogenesis was obviously abnormal after 72 h in culture (*D*) compared with control kidneys treated with sheep preimmune IgGs for 24 (*A*) or 72 h (*C*). Pictures of whole mount kidneys are representative of 22 experiments. Bar: (*A*, *B*, and *D*) 125 μm; (*C*) 200 μm.

sion of the ureter bud and is also needed for further divisions occurring after induction.

Identification of type IV collagenases produced by 11-d kidneys in vivo as MMP2 (Collier et al., 1988) and MMP9 (Wilhelm et al., 1989) was based on their reactivity with specific antibodies and on their ability to degrade gelatin and type IV collagen by zymography. First, by whole mount scanning laser confocal microscopy, MMP2 and MMP9 were observed in mesenchyme throughout the kidney from the superficial to inner areas. They were expressed in the cytoplasmic compartment with a vesicular and perinuclear localization. A comparable cytoplasmic staining pattern was previously described for MMP2 in many human tumors (Mignatti and Rifkin, 1993; Stetler-Stevenson et al., 1993). As a result of this cell distribution, we paid special attention to negativity of controls that consisted in either preimmune serum of the same rabbit (MMP9) or sheep IgGs (MMP2). Second, MMP2 and MMP9 enzymatic activities were also detected by zymography of lysates of 11-d kidney explants. In previous in situ hybridization studies, MMP2 mRNA was observed in 14-d kidney mesenchymal cells (Reponen et al., 1992). In contrast, the search for MMP9 mRNA was negative. In studies performed by Reponen et al. (1994), MMP9 was confined to the tooth and skeletal system during embryogenesis, and it could not be detected above background level in kidney from day 12 onward. Canete-Soler et al. (1995) demonstrated MMP9 mRNA expression in a broader range of embryonic tissues, but still not in embryonic kidney. The discrepancy between our MMP9 protein study and previous MMP9 mRNA studies remains to be elucidated. It has also been observed for MMP2 in lung development (Ganser et al., 1991; Reponen et al., 1992). However, it is well known that mRNA steady state level may change as a function of the developmental or differentiating state of the cells (Trugnan et al., 1995). Moreover, the discordant results may also be explained by the different levels of sensitivity of zymography and immunofluorescence, on the one hand, and of in situ hybridization on the other hand.

As expected from the in vivo data, 11-d embryonic kidneys grown for 24 h in organotypic culture secreted MMP2 and MMP9 in culture medium. Analysis of 24-h conditioned media of mesenchyme and ureter bud dissected apart showed that, as in vivo, both enzymes were produced by mesenchymal cells. A faint band, with the molecular mass of MMP2, was also observed in ureter bud conditioned medium. It might result from a small mesenchymal contamination during dissection, but we cannot exclude from scanning laser confocal microscopy that MMP2 was faintly expressed in the ureter bud. It is noteworthy that MMP2 and MMP9 were demonstrated more easily in organotypic cultures in 24-h media than in lysates of 11-d kidney explants since 20 explants were required while only

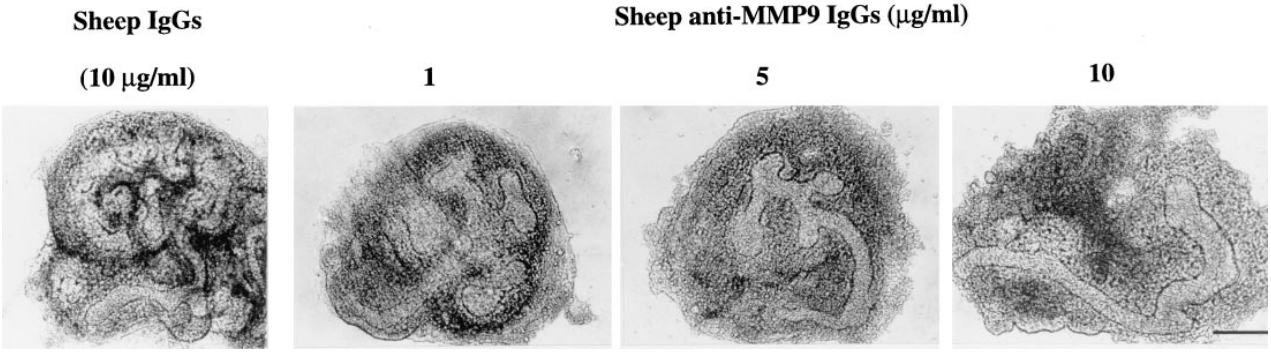

Figure 8. Concentration effect of anti–MMP9 IgGs on branching morphogenesis. Anti–human MMP9 sheep IgGs were added to culture medium for 72 h at concentrations of 1, 5, and 10 μg/ml. Compared with control sheep preimmune IgGs (*10* μg/ml), ureter bud branching was impaired in a concentration-dependent manner by the anti–MMP9 IgGs. It was totally inhibited from a concentration of 10 μg/ml. Abortive branching was observed at 1 μg/ml. Pictures of whole mount kidneys are representative of 22 experiments (see Table I). Bar: (*Sheep IgGs*) 200 μm; (*Sheep anti–MMP9 IgGs 1* and *5*) 150 μm; (*Sheep anti–MMP9 IgGs 10*) 110 μm.

Table I. Number of Kidney Ureter Branching End Buds in Organotypic Cultures Treated with Anti-MMP9 Antibody or TIMP-1

Inhibitor	Concentration of inhibitor		
	1	5	10
		μg/ml	
Sheep anti-MMP9 IgGs ($n = 22$)	8.1 ± 1.6	3.6 ± 0.9	0
Preimmune sheep IgGs ($n = 22$)	ND	ND	13.3 ± 1.5
rhTIMP1 ($n = 13$)	5.0 ± 1.2	2.7 ± 0.7	0
BSA ($n = 13$)	ND	ND	14.0 ± 1.0

Sheep anti–MMP9 IgGs and human recombinant TIMP were added for 72 h to culture media of 11-d kidneys at concentrations of 1, 5, and 10 μg/ml. Controls were sheep preimmune IgGs and BSA (10 μg/ml), respectively. Anti-MMP9 IgGs and TIMP1 reduced, in a concentration-dependent manner, the number of branching end buds (expressed as mean ± SD).

two kidneys secreted enough enzyme for zymographic detection. This suggested that both enzymes were mostly secreted, in line with studies performed in culture on the characterization of metalloproteinase and on their induction by oncogenes (Collier et al., 1988; Wilhelm et al., 1989; Marshall et al., 1993; Knowlden et al., 1995). Interestingly, the 60-kD active form of MMP2 was secreted in culture medium. We could not detect by zymography or Western blotting cleaved active forms of MMP9, but the morphogenetic effects of the anti–MMP9 IgGs and of exogenous TIMP1 suggest that they do exist.

Since in organotypic cultures of 11-d kidneys the pattern and the cellular source of type IV collagenases were similar to those established in vivo, we considered that this in vitro model was relevant and appropriate to investigate the role of MMP2 and MMP9 in the first events of kidney morphogenesis. Culture medium of 11-d embryonic kidneys was therefore supplemented with specific antibodies directed against MMP2 or MMP9 or with hrTIMP1. Anti–MMP2 IgGs had no effect on kidney development. This was not due (*a*) to the lack of antibody penetration in the kidney explant (shown by immunofluorescence of permeabilized kidney); (*b*) to the lack of activation of the enzyme since a 60-kD form comigrating with the major band induced by APMA was present in vivo in lysates of kidney explants and in vitro in conditioned media from whole kidney explant and from mesenchyme; or (*c*) to the specificity of anti–MMP2 antibody since it recognized mouse MMP2 by Western blotting and it inhibited mouse MMP2 enzymatic activity. In contrast, the addition of anti–MMP9 IgGs or of exogenous hrTIMP1 impaired both ureter bud branching and nephron formation. This effect was concentration dependent, irreversible, and still observed after the initial inductive events.

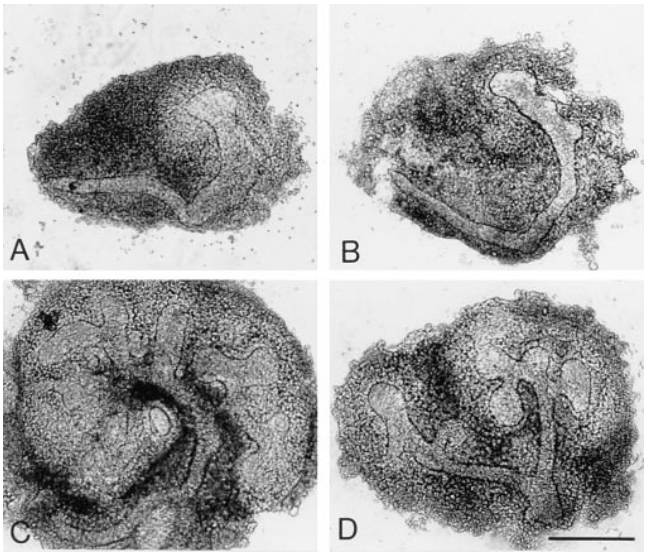

Figure 9. Alterations of 11-d kidney development induced by anti–MMP9 IgGs are not reversible (*A* and *B*) and are still observed after mesenchymal induction (*C* and *D*). (*A* and *C*) Control kidneys incubated with sheep anti–MMP9 IgGs (1 μg/ml) for 24 h only (*A*) or grown in control medium supplemented with sheep IgGs isolated from preimmune serum (1 μg/ml) for 72 h (*C*). (*B* and *D*) Kidneys were either first treated with sheep anti–MMP9 IgGs (1 μg/ml) for 24 h as in (*A*) and then shifted to control medium supplemented with sheep IgGs isolated from preimmune serum (1 μg/ml) for another 48 h (*B*), or grown for 24 h in control medium supplemented with sheep preimmune IgGs (1 μg/ml) and then transferred to medium supplemented with anti–MMP9 IgGs (1 μg/ml) for the next 48 h (*D*). Bar: (*A*, *B*, and *D*) 160 μm; (*C*) 200 μm.

The role of matrix metalloproteinases in branching morphogenesis has long been suspected, but it has been shown in very few instances. It was first reported that interstitial collagenases decreased, but a collagenase inhibitor increased branching of 12-d immature salivary glands (Nakanishi et al., 1986). Second, in transgenic mice that specifically overexpressed stromelysin-1 in mammary gland under the control of the whey acidic protein (WAP) promoter, low levels of expression of the transgene in virgin females induced supernumerary branches of the primary ducts, whereas high levels of expression favored involution of the lactating mammary gland (Sympson et al., 1994). Furthermore, in other experiments by the same group, involution of the mammary gland was delayed by local high concentration of TIMP induced by surgically implanted slow-release pellets (Talhouk et al., 1992). Third, enhanced MMP2 expression in response to exogenous TGFα and EGF inhibited branching morphogenesis in the developing lung (Ganser et al., 1991). Fourth, we now show that branching morphogenesis of the ureter bud requires functional MMP9 activity. Taken as a whole, these results suggest that an appropriate metalloproteinase/TIMP balance is required for branching morphogenesis. This morphogenetic process is complex and can be inhibited in different ways as shown by studies in submandibular gland using anti-laminin and anti–α6 integrin antibodies (Kadoya et al., 1995). It requires both elongation and division steps and is controlled by several metanephric mesenchyme-derived growth factors such as the glial cell

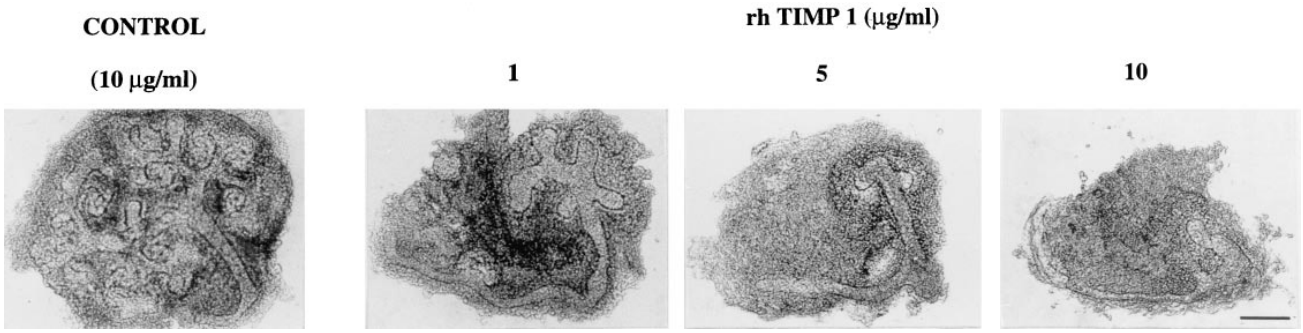

Figure 10. Concentration effect of recombinant human TIMP1 on branching morphogenesis. Recombinant human TIMP1 was added for 72 h at concentrations of 1–10 μg/ml to culture media of 11-d kidneys. Compared with kidneys incubated with 10 μg/ml BSA, ureter bud branching was impaired in a concentration-dependent manner by TIMP1. It was totally inhibited at 10 μg/ml. Pictures of whole mount kidneys are representative of 13 experiments (see Table I). Bar, 140 μm.

line–derived neurotrophic factor (Moore et al., 1996; Pichel et al., 1996; Sanchez et al., 1996), a ligand of the ureter bud orphan tyrosine kinase receptor c-Ret (Treanor et al., 1996). Each step can be independently regulated, since ureter bud elongation and division can be induced by hepatocyte growth factor and PMA, a protein kinase activator, respectively (Davies et al., 1995). Further studies are needed to determine whether MMP9 stimulates ureter bud elongation or division or both.

Since MMP9 is secreted as a proenzyme by mesenchymal cells, it must be activated by proteolytic cleavage to exert its morphogenetic effects. Good candidates for pro-MMP9 activation are serine proteases such as plasmin produced by plasminogen activators, either tissue type (t-PA) or urokinase-like (u-PA). Both were detected in 15.5-d embryonic kidneys by in situ hybridization. Interestingly, t-PA is produced by collecting duct cells in adult kidney (Sappino et al., 1991). Since these cells originate from the ureter bud, it is possible that the ureter bud is a source of t-PA at early stages of renal development that may activate pro-MMP9 around the ureter bud tips.

The mechanisms whereby MMP9 induces branching morphogenesis remain speculative. They may first involve degradation of type IV collagen, denatured collagen, or type XIV collagen, a newly described member of the fibril-associated collagens with interrupted triple helices (FACITS) that has been localized to various embryonic tissues (Sires et al., 1995). Alternatively, the proteolytic activity of MMP9 may not be limited to collagen molecules since it has been shown to cleave the extracellular collagenous domain of 180-kD bullous pemphigoid autoantigen, a transmembrane molecule of the epidermal hemidesmosome (Stähle-Bäckdahl et al., 1994). MMP9 may also be implicated in the processing of growth factor or cytokine precursors (Gearing et al., 1994). Finally, it may regulate branching morphogenesis by favoring the release of matrix-associated growth factors (Flaumenhaft and Rifkin, 1992) or the shedding of protein ectodomains of growth factor or growth factor receptors (Arribas et al., 1996). On the other hand, it remains to be understood why MMP2 inhibition by specific antibodies did not interfere with ureter bud branching although the enzyme was produced and secreted in active form and the antibodies inhibited enzyme activity.

In conclusion, this study demonstrates the production of type IV collagenases in embryonic kidneys in vivo and a key role of MMP9 in branching morphogenesis in organotypic culture. These results may have important implications not only in renal morphogenesis but also in the development of organs characterized by penetration of an epithelial bud in undifferentiated mesenchyme. Mice with targeted mutation or disruption of the MMP9 gene would be helpful to confirm these results in vivo, although MMP9 gene alterations might be lethal since MMPs play a critical role during decidualization (Alexander et al., 1996) or might lead to no phenotype because of compensatory mechanisms.

We thank Dr. E. Lehtonen and Mrs. U. Kiiski (University of Helsinki, Finland) for their help in 11-d kidney dissection, Drs. P. Zaoui and F. Morel (Centre Hospitalier Universitaire de Grenoble, France) for the generous gift of anti-MMP9 antibody, Dr. T. Gilbert for advice in immunomorphology, and M. Delauche and M.C. Verpont for technical assistance in histochemistry.

This work was supported by grants from the Association pour la Recherche sur le Cancer (1303) and from the Secrétariat d'Etat à la Recherche (ACC-SV #4).

Received for publication 12 February 1996 and in revised form 7 January 1997.

References

Alexander, C.M., E.J. Hansell, O. Behrendtsen, M.L. Flannery, N.S. Kishnani, S.P. Hawkes, and Z. Werb. 1996. Expression and function of matrix metalloproteinases and their inhibitors at the maternal-embryonic boundary during mouse embryo implantation. *Development (Camb.).* 122:1723–1736.

Apte, S.S., K. Hayashi, M.F. Seldin, M.-G. Matei, M. Hayashi, and B.R. Olsen. 1994. Gene encoding a novel murine tissue inhibitor of metalloproteinases (TIMP), TIMP3, is expressed in developing mouse epithelia, cartilage, and muscle, and is located on mouse chromosome 10. *Dev. Dyn.* 200:177–197.

Arribas, J., L. Coodly, P. Vollmer, T.K. Kishimoto, S. Rose-John, and J. Massagué. 1996. Diverse cell surface protein ectodomains are shed by a system sensitive to metalloprotease inhibitors. *J. Biol. Chem.* 271:11376–11382.

Bard, J.B.L. 1990. The Cellular and Molecular Processes of Developmental Anatomy. Cambridge University Press, Cambridge, UK. 291 pp.

Brenner, C.A., R.R. Adler, D.A. Rappolee, R.A. Pederson, and Z. Werb. 1989. Genes for extracellular matrix-degrading metalloproteinases and their inhibitor, TIMP, are expressed during early mammalian development. *Genes & Dev.* 3:848–859.

Canete-Soler, R., Y.-H. Gui, K.K. Linask, and R. Muschel. 1995. Developmental expression of MMP-9 (Gelatinase B) mRNA in mouse embryos. *Dev. Dyn.* 204:30–40.

Cawston, T.E., W.A. Galloway, E. Mercer, G. Murphy, and J.J. Reynolds. 1981. Purification of rabbit bone inhibitor of collagenase. *Biochem. J.* 195:159–165.

Collier, I.E., S.M. Wilhelm, A.Z. Eisen, B.L. Marmer, G.A. Grant, J.L. Seltzer, A. Kronberger, C. He, E.A. Bauer, and G.I. Goldberg. 1988. H-ras onco-

gene-transformed human bronchial epithelial cells (TBE) secrete a single metalloprotease capable of degrading basement membrane collagen. *J. Biol. Chem.* 263:6579–6587.

Davies, J., M. Lyon, J. Gallager, and D. Garrod. 1995. Sulphated proteoglycan is required for collecting duct growth and branching but not nephron formation during kidney development. *Development (Camb.).* 121:1507–1517.

De Clerk, Y.A., T.-D. Yean, B.J. Ratzkin, H.S. Lu, and K.E. Langley. 1989. Purification and characterization of two related but distinct metalloproteinase inhibitors secreted by bovine aortic endothelial cells. *J. Biol. Chem.* 264: 17445–17453.

Ekblom, P. 1993. Basement membrane in development. *In* Molecular and Cellular Aspects of Basement Membranes. D.H. Rohrbach and R. Timpl, editors. Academic Press, Inc., San Diego, CA. 359–383.

Ekblom, P., I. Thesleff, A. Miettinen, and L. Saxen. 1981. Organogenesis in a defined medium supplemented with transferrin. *Cell Differ.* 10:281–288.

Flaumenhaft, R., and D.B. Rifkin. 1992. The extracellular regulation of growth factor action. *Mol. Biol. Cell.* 3:1057–1065.

Ganser, G.L., G.P. Stricklin, and L.M. Matrisian. 1991. EGF and TGFα influence in vitro lung development by the induction of matrix-degrading metalloproteinases. *Int. J. Dev. Biol.* 35:453–461.

Gearing, A.J.H., P. Beckett, M. Christodoulou, M. Churchill, J. Clements, A.H. Davidson, A.H. Drummond, W.A. Galloway, R. Gilbert, J.L. Gordon, et al. 1994. Processing of tumor necrosis factor-α precursor by metalloproteinases. *Nature (Lond.).* 370:555–557.

Goldberg, G.I., B.L. Marmer, G.A. Grant, A.Z. Eisen, A. Wilhelm, and C. He. 1989. Human 72-kDa type IV collagenase forms a complex with a tissue inhibitor of metalloproteinases designated TIMP-2. *Proc. Natl. Acad. Sci. USA.* 86:8207–8211.

Harvey, M.B., K.J. Leco, M.Y.A. Arcellana-Panlilio, X. Zhang, D.R. Edwards, and G.A. Schultz. 1995. Proteinase expression in early mouse embryos is regulated by leukaemia inhibitory factor and epidermal growth factor. *Development (Camb.).* 121:1005–1014.

Heussen, C., and E.B. Dowdle. 1980. Electrophoretic analysis of plasminogen activators in polyacrylamide gels containing sodium dodecyl sulfate and copolymerized substrates. *Anal. Biochem.* 102:196–202.

Hipps, D.S., R.M. Hembry, A.J.P. Docherty, J.J. Reynolds, and G. Murphy. 1991. Purification and characterization of human 72 kDa gelatinase (type IV collagenase). Use of immunolocalisation to demonstrate the non-coordinate regulation of the 72-kDa and 95-kDa gelatinases by human fibroblasts. *Biol. Chem. Hoppe-Seyler.* 372:287–296.

Kadoya, Y., K. Kadoya, M. Durbeej, K. Holmvall, L. Sorokin, and P. Ekblom. 1995. Antibodies against domain E3 of laminin-1 and integrin α6 subunit perturb branching epithelial morphogenesis of submandibular gland, but by different modes. *J. Cell Biol.* 129:521–534.

Knowlden, J., J. Martin, M. Davies, and J. Williams. 1995. Metalloproteinase generation by human glomerular epithelial cells. *Kidney Int.* 47:1682–1689.

Lefebvre, O., C. Régnier, M.P. Chenard, C. Wendling, P. Chambon, P. Basset, and M.C. Rio. 1995. Developmental expression of mouse stromelysin-3 mRNA. *Development (Camb.).* 121:947–955.

Lim, M., F. Elfman, A. Dohrman, G. Cunha, and C. Basbaum. 1995. Upregulation of the 72-kDa type IV collagenase in epithelial and stromal cells during rat tracheal gland morphogenesis. *Dev. Biol.* 171:521–530.

Marshall, B.C., A. Santana, Q.-P. Xu, M.J. Petersen, E.J. Campbell, J.R. Hoidal, and H.G. Welgus. 1993. Metalloproteinases and tissue inhibitor of metalloproteinases in mesothelial cells. *J. Clin. Invest.* 91:1792–1799.

Mignatti, P., and D.B. Rifkin. 1993. Biology and biochemistry of proteinases in tumor invasion. *Physiol. Rev.* 73:161–195.

Moore, M., R.D. Klein, I. Farinas, H. Sauer, M. Armanini, H. Phillips, L.F. Reichardt, A.M. Ryan, K. Carver-Moore, and A. Rosenthal. 1996. Renal and neuronal abnormalities in mice lacking GDNF. *Nature (Lond.).* 382:76–79.

Morel, F., S. Berthier, M. Guillot, P. Zaoui, C. Massoubre, F. Didier, and P.V. Vignais. 1993. Human neutrophil gelatinase is a collagenase type IV. *Biochem. Biophys. Res. Commun.* 191:269–274.

Murphy, G., J.J. Reynolds, U. Bretz, and M. Baggiolini. 1982. Partial purification of collagenase and gelatinase from human polymorphonuclear leukocytes. Analyses of their actions on soluble and insoluble collagens. *Biochem. J.* 253:209–221.

Murphy, G., R. Ward, R.M. Hembry, J.J. Reynolds, K. Khun, and K. Tryggvason. 1989. Characterization of gelatinase from pig polymorphonuclear leukocytes. A metalloproteinase resembling tumor type IV collagenase. *Biochem. J.* 258:463–472.

Nakanishi, Y., F. Suguira, J.I. Kishi, and T. Hayakawa. 1986. Collagenase inhibitor stimulates cleft formation during early morphogenesis of mouse salivary gland. *Dev. Biol.* 113:201–206.

Nomura, S., B.L. Hogan, A.J. Wills, J.K. Heath, and D.R. Edwards. 1989. Developmental expression of tissue inhibitor of metalloproteinase (TIMP) RNA. *Development (Camb.).* 105:575–583.

Okada, Y., Y. Gonoji, K. Naka, K. Tomita, I. Nakanishi, K. Iwata, K. Yamashita, and T. Hayakawa. 1992. Matrix metalloproteinase 9 (92 kDa gelatinase/type IV collagenase) from HT 1080 human fibrosarcoma cells. *J. Biol. Chem.* 267: 21712–21719.

Pichel, J.G., L. Shen, H.Z. Sheng, A.-C. Granholm, J. Drago, A. Grinberg, E.J. Lee, S.P. Huang, M. Saarma, B.J. Hoffer, et al. 1996. Defects in enteric innervation and kidney development in mice lacking GDNF. *Nature (Lond.).* 382:73–76.

Reponen, P., C. Sahlberg, P. Huhtala, T. Hurskainen, I. Thesleff, and K. Tryggvason. 1992. Molecular cloning of murine 72-kD type IV collagenase and its expression during mouse development. *J. Biol. Chem.* 267: 7856–7862.

Reponen, P., C. Sahlberg, C. Munaut, I. Thesleff, and K. Tryggvason. 1994. High expression of the 92-kD type IV collagenase (gelatinase B) in the osteoclast lineage during mouse development. *J. Cell Biol.* 124:1091–1102.

Reponen, P., I. Leivo, C. Sahlberg, S.S. Apte, B.R. Olsen, I. Thesleff, and K. Tryggvason. 1995. 92-kD type IV collagenase and TIMP-3, but not 72-kDa type IV collagenase or TIMP-1 or TIMP-2, are highly expressed during mouse embryo implantation. *Dev. Dyn.* 202:388–396.

Richter, A., K.K. Sanford, and V.J. Evans. 1972. Influence of oxygen and culture media on plating efficiency of some mammalian tissue cells. *J. Natl. Cancer Inst.* 49:1705–1712.

Sanchez, M.P., I. Silos-Santiago, J. Frisen, B. He, S.A. Lira, and M. Barbacid. 1996. Renal agenesis and the absence of enteric neurons in mice lacking GDNF. *Nature (Lond.).* 382:70–73.

Sappino, A.-P., J. Huarte, J.-D. Vassalli, and D. Belin. 1991. Sites of synthesis of urokinase and tissue-type plasminogen activators in the murine kidney. *J. Clin. Invest.* 87:962–970.

Sires, U.I., B. Dublet, E. Aubert-Foucher, M. van der Rest, and H.G. Welgus. 1995. Degradation of the COL1 domain of type XIV collagen by 92-kD gelatinase. *J. Biol. Chem.* 270:1062–1067.

Stähle-Bäckdahl, M., M. Inoue, G.J. Giudice, and W.C. Parks. 1994. 92-kD gelatinase is produced by eosinophils at the site of blister formation in bullous pemphigoid and cleaves the extracellular domain of recombinant 180-kD bullous pemphigoid autoantigen. *J. Clin. Invest.* 93:2022–2030.

Stetler-Stevenson, W.G., S. Aznavoorian, and L.A. Liotta. 1993. Tumor cell interactions with the extracellular matrix during invasion and metastasis. *Annu. Rev. Cell Biol.* 9:541–573.

Sympson, C.J., R.S. Talhouk, C.M. Alexander, J.R. Chin, S.M. Clift, M.J. Bissel, and Z. Werb. 1994. Targeted expression of stromelysin-1 in mammary gland provides evidence for a role of proteinases in branching morphogenesis and the requirement for an intact basement membrane for tissue-specific gene expression. *J. Cell Biol.* 125:681–693.

Talhouk, R.S., M.J. Bissel, and Z. Werb. 1992. Coordinated expression of extracellular matrix-degrading proteinases and their inhibitors regulates mammary epithelial function during involution. *J. Cell Biol.* 118:1271–1282.

Treanor, J.J.S., L. Goodman, F. de Sauvage, D.M. Stone, K.T. Poulsen, C.D. Beck, C. Gray, M.P. Armanini, R.A. Pollock, F. Hefti, et al. 1996. Characterization of a multicomponent receptor for GDNF. *Nature (Lond.).* 382:80–83.

Trugnan, G., L. Baricault, F. David, M. Garcia, and C. Sapin. 1995. Control of Dipeptidylpeptidase IV by CD 26. Cell surface expression in intestinal cells. In Dipeptidylpeptidase IV (CD 26) in Metabolism and the Immune Response. D. Fleischer, editor. R.G. Landus Company, Austin, TX. 79–98.

Werb, Z., C.M. Alexander, and R.R. Adler. 1992. Expression and function of matrix metalloproteinases in development. *Matrix Suppl.* 1:337–343.

Wilhelm, S.M., I.E. Collier, B.L. Marmer, A.Z. Eisen, G.A. Grant, and G.I. Goldberg. 1989. SV40-transformed human lung fibroblasts secrete a 92-kDa type IV collagenase which is identical to that secreted by normal human macrophages. *J. Biol. Chem.* 264:17213–17221.